Cell

Structural Analysis of *E. coli* hsp90 Reveals Dramatic Nucleotide-Dependent Conformational Rearrangements

Andrew K. Shiau,[1,2,4] Seth F. Harris,[1,3,4] Daniel R. Southworth,[1] and David A. Agard[1,*]
[1] Howard Hughes Medical Institute and Department of Biochemistry and Biophysics, University of California, San Francisco, San Francisco, CA 94158, USA
[2] Department of Biology, Kalypsys, Inc., 10420 Wateridge Circle, San Diego, CA 92121, USA
[3] Roche Palo Alto, 3431 Hillview Avenue, Palo Alto, CA 94304, USA
[4] These authors contributed equally to this work.
*Contact: agard@msg.ucsf.edu
DOI 10.1016/j.cell.2006.09.027

SUMMARY

In eukaryotes, the ubiquitous and abundant members of the 90 kilodalton heat-shock protein (hsp90) chaperone family facilitate the folding and conformational changes of a broad array of proteins important in cell signaling, proliferation, and survival. Here we describe the effects of nucleotides on the structure of full-length HtpG, the *Escherichia coli* hsp90 ortholog. By electron microscopy, the nucleotide-free, AMPPNP bound, and ADP bound states of HtpG adopt completely distinct conformations. Structural characterization of nucleotide-free and ADP bound HtpG was extended to higher resolution by X-ray crystallography. In the absence of nucleotide, HtpG exhibits an "open" conformation in which the three domains of each monomer present hydrophobic elements into the large cleft formed by the dimer. By contrast, ADP binding drives dramatic conformational changes that allow these hydrophobic elements to converge and shield each other from solvent, suggesting a mechanism by which nucleotides could control client protein binding and release.

INTRODUCTION

Several families of heat shock proteins are molecular chaperones that assist protein folding in vivo. These enzymes bind to exposed hydrophobic surfaces of their client proteins, thereby preventing nonspecific intermolecular interactions that could lead to aggregation. Subsequent ATP-mediated dissociation provides client proteins the opportunity to proceed down their folding pathways (Young et al., 2004). Different heat shock proteins are required at different stages of folding. Members of the 70 kilodalton (hsp70) and the 60 kilodalton (GroEL) families facilitate the early stages of polypeptide folding, binding linear chains (Zhu et al., 1996) and "molten globules" (Horst et al., 2005), respectively. In contrast, members of the ubiquitous and abundant 90 kilodalton heat-shock protein (hsp90) family appear to associate with client proteins at their latest stages of folding (Freeman and Yamamoto, 2002; Young et al., 2001), (Picard, 2002; Pratt and Toft, 2003; Richter and Buchner, 2001; Zhao et al., 2005). In mammalian cells, hsp90 forms complexes with the quiescent forms of a wide array of cellular signaling proteins and chaperones the conformational changes essential for their signaling-dependent activities, including ligand binding and association with partner proteins. Hence, hsp90 plays a unique role in cellular physiology by preferentially stabilizing near-native state structures and aiding the dynamic assembly and disassembly of signaling complexes. Since many hsp90 client proteins play critical roles in cellular proliferation and survival, pharmacologic suppression of hsp90 activity, and hence the many hsp90-dependent signaling pathways, blocks growth of cancerous cells (Whitesell and Lindquist, 2005). As a consequence, hsp90 inhibitors such as certain analogs of geldanamycin are currently in clinical trials for treatment of numerous malignancies (Chiosis et al., 2003; Neckers and Ivy, 2003; Workman, 2004).

Structure/function studies of hsp70 and GroEL have established a common mechanistic theme in which ATP binding and hydrolysis trigger conformational changes that alter the hydrophobicity of domains used to engage client proteins (Feltham and Gierasch, 2000; Grantcharova et al., 2001; Mayer and Bukau, 2005; Young et al., 2004). Similarly, biochemical and genetic data indicate that ATPase activity and surface hydrophobicity are also key factors that control client protein association (Richter and Buchner, 2001; Young et al., 2001). X-ray crystal structures of the three independent domains of hsp90 (the amino-terminal domain (NTD; Jez et al., 2003; Prodromou et al., 1997; Stebbins et al., 1997), the middle domain (MD; Meyer

et al., 2003), and the carboxy-terminal domain (CTD; Harris et al., 2004) from various species as well as that of an NTD/MD fragment (Huai et al., 2005) of the *Escherichia coli* hsp90, HtpG, have facilitated identification of structural elements involved in ATP binding/hydrolysis and others potentially important for client protein binding. Further, structures of inhibitor complexes of the yeast and human hsp90 NTDs have indicated that these compounds block ATPase activity, and hence hsp90 function, at least in part by occupying the nucleotide binding site contained within the NTD and preventing ATP access (Dymock et al., 2005; Jez et al., 2003; Roe et al., 1999; Stebbins et al., 1997). Finally, a recent structure of a full-length yeast hsp90, hsc82, bound to AMPPNP and the cochaperone p23 (Ali et al., 2006) confirms that ATP hydrolysis requires NTD dimerization and the presence of an NTD/MD composite active site. However, a unified, structurally validated mechanism linking hsp90 ATPase activity and client protein binding is lacking.

To address this issue, we have examined the impact of nucleotide binding on HtpG via electron microscopy and X-ray crystallography. In electron micrographs, HtpG adopts three different conformational states in the absence of nucleotide and when bound to AMPPNP and ADP. The size and shape of AMPPNP bound HtpG is consistent with the structure of the AMPPNP bound yeast hsc82:p23 complex (Ali et al., 2006), indicating a conserved structural role for ATP binding. To further characterize the remaining two states, for which there is no high-resolution structural information, we have determined the X-ray crystal structures of intact HtpG with and without ADP. Our refinement and interpretation of these medium resolution structures (~3.5–3.6 Å) has been enabled by our new high-resolution structure determinations of the NTD (1.65 Å) and the MD (1.90 Å) and our previously reported CTD structure (Harris et al., 2004). In agreement with the data from electron microscopy, the HtpG dimer in the absence of nucleotide adopts an "open" conformation in which the positioning of the two monomers creates a large central cleft lined by hydrophobic elements from each of the three domains. In contrast, ADP binding stabilizes a radically different domain organization within each monomer that leads to a narrowing of the cleft. The effect of these motions on the dimer, coupled with modeling, suggests a mechanism by which ADP binding could bring together and bury the hydrophobic regions exposed in the apo state, leading to client protein release. These concepts lead us to propose a structurally based model for the hsp90 chemomechanical cycle. Given the high degree of sequence and structural conservation among family members, these mechanisms should apply to both prokaryotic and eukaryotic hsp90s.

RESULTS

Electron Microscopy Reveals Three Distinct HtpG Conformational States

The general picture that has emerged from structural studies of the hsp60 and hsp70 molecular chaperones as well as other GHKL family members (a superfamily composed of gyrase, hsp90, histidine kinases, and MutL; Dutta and Inouye, 2000) is that nucleotide binding and hydrolysis drives an interconversion between two stable conformational states. Previously, low-angle rotary-shadowing electron microscopy (EM) has provided evidence for ATP-dependent conformational changes in human hsp90 (Maruya et al., 1999). To investigate this further, we have used negative-stain EM combined with single-particle class averaging to examine nucleotide-dependent conformational states in HtpG. Class averaging allows the identification and averaging of two-dimensional projection images from large numbers of individual particles, resulting in a much more reliable view of molecular shape. From fields of single particles (Figure S1) HtpG clearly assumes at least three distinct states. Representative single particle images and class averages reveal that in the absence of nucleotide HtpG predominantly adopts an open "V" shape (Figure 1a). From the particle images, it is readily apparent that the opening angle is quite variable, indicating that the apo conformation is flexible. By contrast, AMPPNP and ADP binding stabilize two very different and far more discrete states. AMPPNP bound HtpG forms a closed, elongated shape. Using reference-free class averaging and projection matching methods, AMPPNP bound HtpG is similar in both size and detailed shape to the yeast hsc82:p23:AMPPNP crystal structure (Ali et al., 2006) (Figure 1b). HtpG apparently does not require cochaperone binding to stabilize this conformation. Unexpectedly, in the presence of ADP, HtpG adopts a significantly more compact, globular conformation (Figure 1c). This novel conformation is suggestive of a third unanticipated state in the hsp90 nucleotide-dependent chaperone cycle.

Structure of the Unliganded Full-Length HtpG

To extend the EM analysis, the structure of full-length unliganded HtpG was solved at 3.5 Å resolution using multiple isomorphous replacement phasing techniques. Model building (current R/R_{free} = 32.9%/37.0%, Tables S1 and S2) was greatly facilitated by heavy atom sequence markers (see Supplemental Experimental Procedures) and the high-resolution structures of the individual domains (Table S1, Figures S2 and S3; Harris et al., 2004). Consistent with solution studies, intact HtpG forms a dimer in the crystal. Viewed from one angle, this dimer resembles a twisted, two-bladed propeller ~70 Å tall and ~150 Å wide (Figure 2). The overall shape and dimensions are consistent with those derived from our HtpG electron micrographs and those of human hsp90 (Maruya et al., 1999). Like other members of the hsp90 family, each HtpG monomer can be divided into three domains, the NTD (residues 1–227), MD (residues 233–489), and CTD (residues 501–624). The NTD is composed of an eight-stranded β sheet (strands S2–S9) flanked by eight α helices (H1–H8) (Figure 3A). The MD forms an elongated structure comprised of three subdomains, two αβα sandwiches (residues 233–366; S10–S13 and H9–H11 and

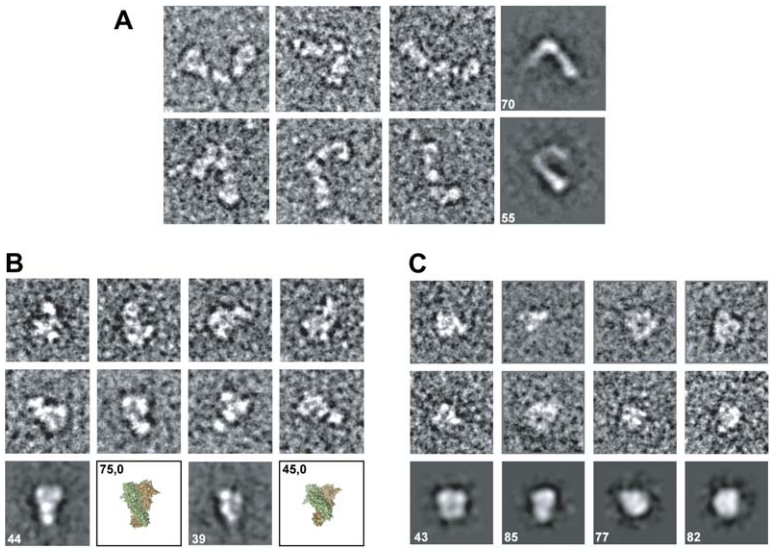

Figure 1. HtpG Adopts Three Distinct Conformational States

(A–C) Representative montage of raw single particle views and reference-free class averages of negatively stained HtpG (fields of particles are shown in Figure S1). In (A), HtpG is incubated in the absence of nucleotide (apo), in (B), it is incubated with AMPPNP, and in (C), it is incubated with ADP. The class averages are shown to the right (A) or at the bottom (B and C) of the raw images, with the number of particles used in each average indicated. All images have a 2.2 Å pixel size (box width is 350 Å for A and 260Å for B and C). To examine the correspondence between the EM images of HtpG:AMPPNP and the yeast crystal structure (Ali et al., 2006), a set of 2D projections were calculated from the hsp82 coordinates and matched to the HtpG:AMPPNP class averages (B, last row). For two representative views, the matching structures are shown to the right of each class average.

residues 401–489; S14–S15 and H15–H19) connected via a small domain consisting of a spiral of three helices (residues 367–400; H12–H14) (Figure S3). The CTD possesses a unique mixed αβ fold (S16–S18 and H20–H24). As suggested by a previously described low-resolution electron-density map (Harris et al., 2004), one NTD is located at the outer tip of each blade, and the MDs form the bulk of the body of the blades. The two CTDs located at the central hub homodimerize via the formation of a four-helix bundle identical to that observed in the isolated CTD dimer (Harris et al., 2004). The buried surface area in the full-length dimer 1280 Å^2 is larger than that of the isolated CTD dimer (930 Å^2), primarily due to interactions between H16 from the third subdomain of the MD with H24 of the CTD from the partner monomer.

Overall, the structures of the three domains in the context of the intact protein are highly similar to those determined in isolation (1.50, 0.73, and 0.83 Å rmsd for the NTD, MD, and CTD respectively; Table S1, Figures 3B and S3, and Harris et al. [2004]). Only two regions of the protein exhibit significant differences, one in the vicinity of helices H1, H3, H4 in the NTD and H21 in the CTD. The deviations in the NTD are related to nucleotide binding and will be discussed in the subsequent section. H21 (H2 of the isolated domain) is an exposed amphipathic helix that is ordered in the isolated CTD dimer but disordered in the full-length structure. However, because unambiguous electron density is present for the residues (541–543 and 565–566) that connect H21 to the second and third strands of the CTD β sheet, the positioning of H21 can be predicted; the linking regions are arranged such that H21 from each monomer would clearly project into the a large cleft formed by the dimer (Figure 2).

Because of the positioning of its exposed hydrophobic face, H21 has been proposed to be a potential client protein binding site (Harris et al., 2004). Another region, centered on a surface loop (residues 281–296) in the MD, has been previously ascribed a similar function. Large, hydrophobic residues important for v-src maturation are on or near the equivalent loop (residues 324–340) in hsp82 (Meyer et al., 2003). This loop in HtpG (referred to as the src loop) exhibits poor sequence conservation but has a similar pattern of hydrophobic and hydrophilic residues. Despite its exposed nature, the structure of this loop is surprisingly invariant across all MD structures (Figure S3), suggesting it may serve a common role in client protein interaction. Consistent with this idea, the src loop, like H21, extends into the dimeric cleft (Figure 2)

Domain Connections and Interfaces Support Flexibility of Apo State

HtpG, like other hsp90s, exhibits significant structural flexibility in the absence of nucleotides (Figure 1). In Grp94, the hsp90 endoplasmic reticulum paralog, and hsp82, a long, repetitive, charged sequence once thought to loosely tether the NTD and MD is actually located within the turn sequence of a β hairpin that completes the central NTD β sheet. Consistent with the NTD/MD HtpG fragment structure, our full-length HtpG structure shows a very similar feature, two β strands (S8 and S9) stabilized by a type I′ turn (Figure 2). As a consequence, the true NTD/MD interdomain linker is only seven residues in length (residues 227–233). This observation, combined with the fact that the NTD/MD interface buries a significant amount of surface area (1060 Å^2), suggests that these domains are not free to move independently.

By contrast, the features of the MD/CTD boundary are strongly suggestive of a dynamic relationship. These two domains are linked by a long, highly mobile tether (residues 490–500, with residues 492–499 being disordered; Figure 2). In addition, the interface between these domains is quite small (320 Å^2) and resembles a ball-and-socket joint (Figure 2). Thus, we believe that the structural flexibility of the apo-state observed by EM (Figures 1a and S1a) is largely due to rigid body motions between the NTD/MD segment and the CTD. This plasticity may be

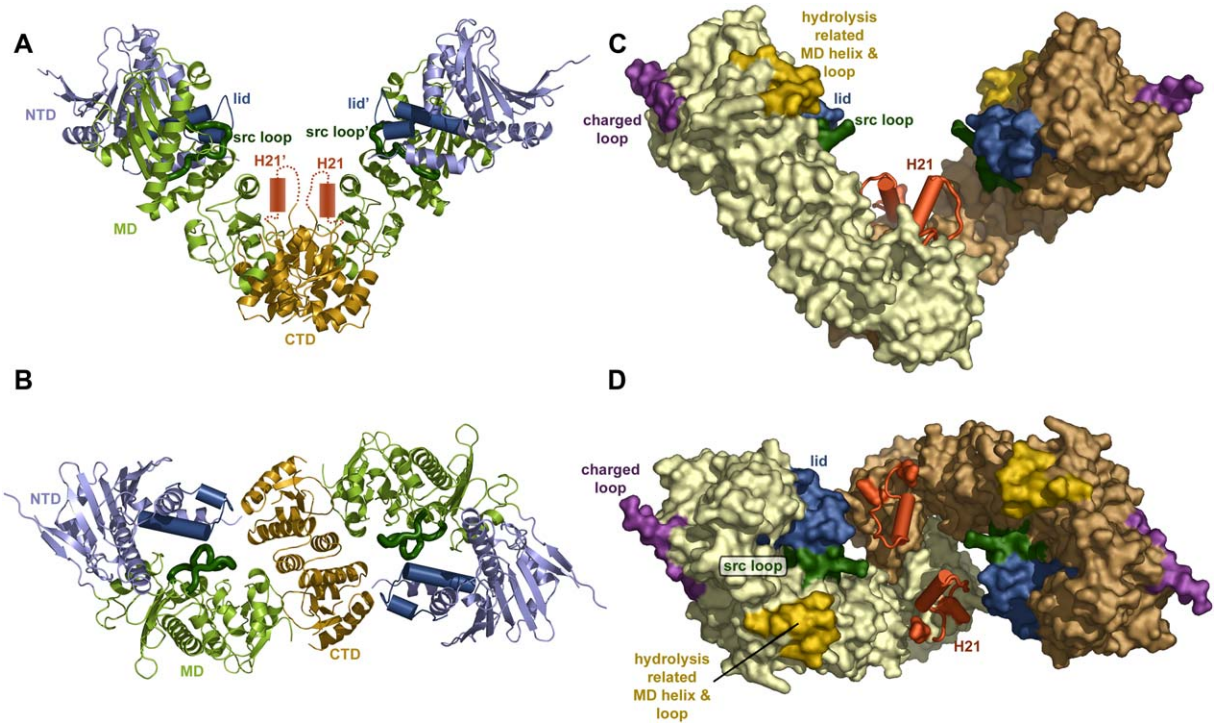

Figure 2. Overall Structure of Apo Full-Length HtpG

(A and B) Two orthogonal ribbon views of the apo full-length dimer. The amino-terminal domain (NTD) (blue) contains the "active-site lid" region (helices H4 and H5; dark blue cylinders). The middle domain (MD) (green) contains the extended "src loop" (dark green tube), and the carboxy-terminal domain (CTD) is shown in gold. The exposed carboxy terminal helices (H21 and H21') (red boxes) are disordered in this structure and are illustrated based on alignment with the isolated CTD structure.

(C and D) Two orthogonal surface views indicating functional regions of the apo full-length dimer. The NTD lid (blue), MD src loop (green), and CTD amphipathic helices (red and modeled as in A) present hydrophobic surfaces into the larger intra-dimer cleft proposed to be important for client-protein binding. Additionally, the surface is colored (purple charged loop) to show the predicted location of the highly charged sequence present in eukaryotic hsp90 but absent in HtpG. The MD loop and helix H10 that contain residues potentially important for ATP hydrolysis (yellow) are also shown.

important for the accommodation of structurally diverse client proteins.

Nucleotide-Mediated Conformational Changes in the NTD Impact Domain Organization

Structures of the isolated eukaryotic hsp90 NTDs reveal that the domain contains a conserved structural element, known as the "active site lid," composed of two helices and the intervening loop that is located immediately adjacent to the ATP binding site (Jez et al., 2003; Prodromou et al., 1997; Stebbins et al., 1997). Interestingly, this potentially functionally important region of htpG (residues 100–126) shares little sequence homology beyond a well-conserved IGQFGVG motif (htpG residues 120–126) to the eukaryotic hsp90s. However, these residues do form a lid-like element in the structure of the HtpG Mg^{2+}ADP NTD complex (1.65 Å; R factor = 16.3%; free R factor = 19.8%; Table S1). As in the yeast and human hsp90 NTDs, the lid is positioned proximal to the ADP binding site with the two lid helices lying in a plane parallel to that of the NTD β sheet (Figure 3B). However, due to its dissimilar sequence, the HtpG lid helices are longer and shifted relative to their eukaryotic counterparts.

Examination of the relative positioning of the NTD and MD in the full-length apo structure (Figure 2), identical to that observed in the NTD/MD fragment structure (Huai et al., 2005), reveals that it would sterically preclude the conformation of the isolated ADP bound NTD (Figures S2 and S4). The key determinant of this conflict is the active site lid (Figure 3A), which, if it were positioned as in the isolated ADP bound NTD (Figure 3B), would collide with elements of the MD first subdomain (including the src loop) (Figure S4B). In both the NTD/MD fragment and the apo full-length structures, this potential steric clash is avoided by significant reorganization of the NTD elements within the vicinity of the lid (Figure S4). The majority of the active site lid in the NTD/MD fragment is disordered and not visible in the structure (Huai et al., 2005). In contrast, the lid in the apo full-length structure adopts a novel configuration in which the plane of the lid lies roughly orthogonal to that of the NTD β sheet (Figure 3A). Helix H1, which abuts the lid in the isolated NTD, pivots at Tyr25 by 35° to lie along one face of the lid. Because this results in the repositioning of Gln15 12.3 Å distant from its position in the isolated NTD structure, the first strand of the NTD core sheet is disrupted, and residues

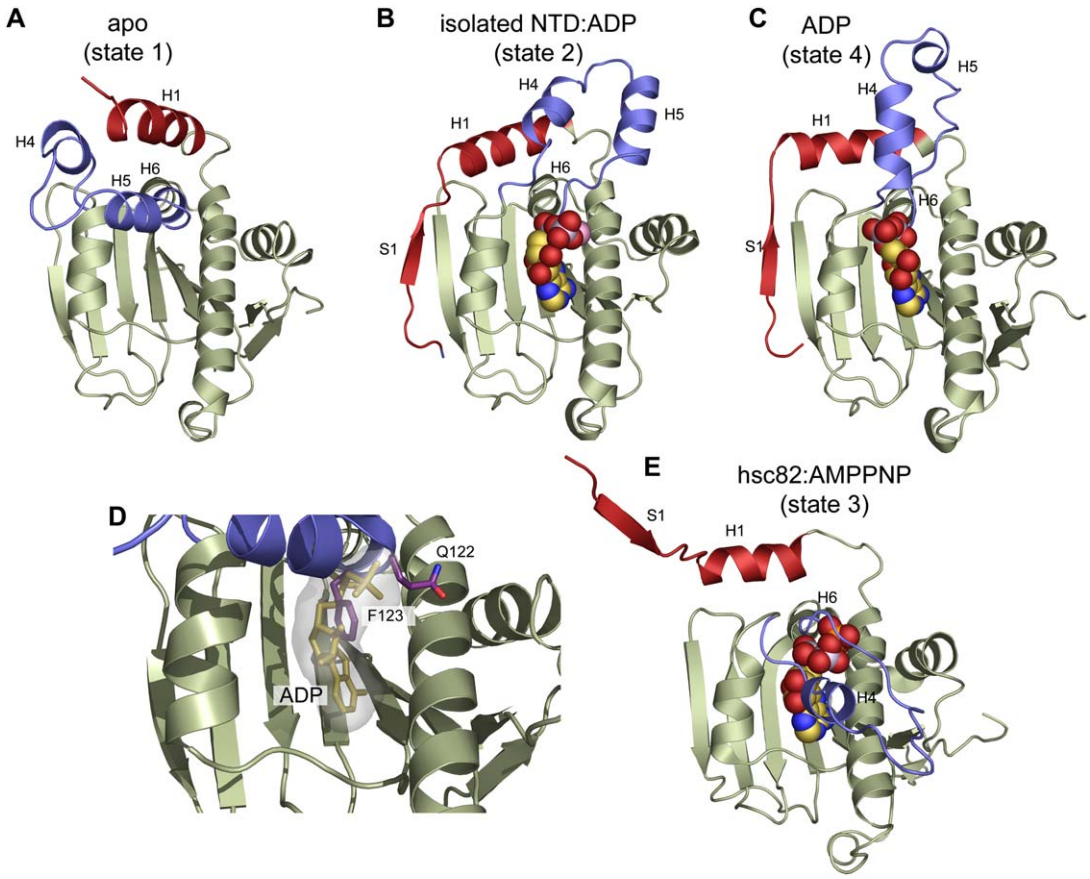

Figure 3. Four Different Conformational States of the NTD; Key Elements Are Strand S1 and Helix H1 (Red) and the Lid (Helices H4 and H5) (Blue)

(A) Ribbon diagram of the NTD in the apo full-length dimer. H5 occludes a portion of the nucleotide binding pocket (see subsequent panels). The amino-terminal residues of the protein (which form S1 in the other structures) are disordered, while H1 is parallel to and packed against the lid helices.

(B) Ribbon diagram of the Mg^{2+}ADP bound isolated NTD. The amino-terminal residues are ordered and form β strand S1 (red). H1 (red) has pivoted by 35° and rolled by 180° from its apo structure. The lid is raised to allow nucleotide binding, and the lid helices are rotated around their primary axes, altering their interaction surface with H1.

(C) Ribbon diagram of the NTD from the ADP bound full-length dimer. H1 and the lid assume a third conformation, which is similar to but distinct from that of the Mg^{2+}ADP bound isolated NTD (B).

(D) Modeling the ADP from the isolated NTD (B) into the apo state (A). The apo state is clearly incompatible with nucleotide binding, because the lid residues Gln122 and Phe123 clash with the ribose and phosphate groups of ADP.

(E) Ribbon diagram of the NTD from the AMPPNP bound yeast hsc82 (Ali et al., 2006). The lid has folded over the nucleotide, while the amino terminus of the protein (S1) is extended to interact with the partner monomer for a strap that stabilizes NTD-NTD dimerization.

1–14 are disordered. In adopting this conformation, the lid and helix H1 do not undergo simple en bloc motions; instead, helix H5 transforms from a 3_{10} helix to an α helix. This, combined with an extension of H5, forces the highly conserved GQFGVG sequence connecting helices H5 and H6 to adopt a kinked helical conformation. Additionally, helix H1 rotates along its axis by ~180° (Figure 4).

In HtpG, conformational changes in the lid have important functional consequences on nucleotide binding. In the apo state, the lid is positioned so as to sterically block nucleotide binding. The mainchain of residues 121–124 (the kink connecting helices H5 and H6) in the full-length structure crosses the region occupied by the α and β phosphates of ADP in the isolated domain structure (Figure 3D). Further, because of the conformational changes within helix H5, the side chain of Phe123 points into the space occupied by the nucleotide sugar and base. This "autoinhibitory" conformation has been also observed in the structures of an HtpG NTD/MD fragment and that of an N-terminal deletion mutant of the yeast protein (Richter et al., 2006). Based on the yeast and human NTD complexes (Roe et al., 1999; Stebbins et al., 1997), the lid position in the full-length structure would also preclude binding of nucleotide-competitive hsp90 inhibitors such as geldanamycin and radicicol.

Overall, our data suggests that binding of nucleotides (and potentially inhibitors) to the NTD can lead to two potential outcomes. It can cause the disordering of the

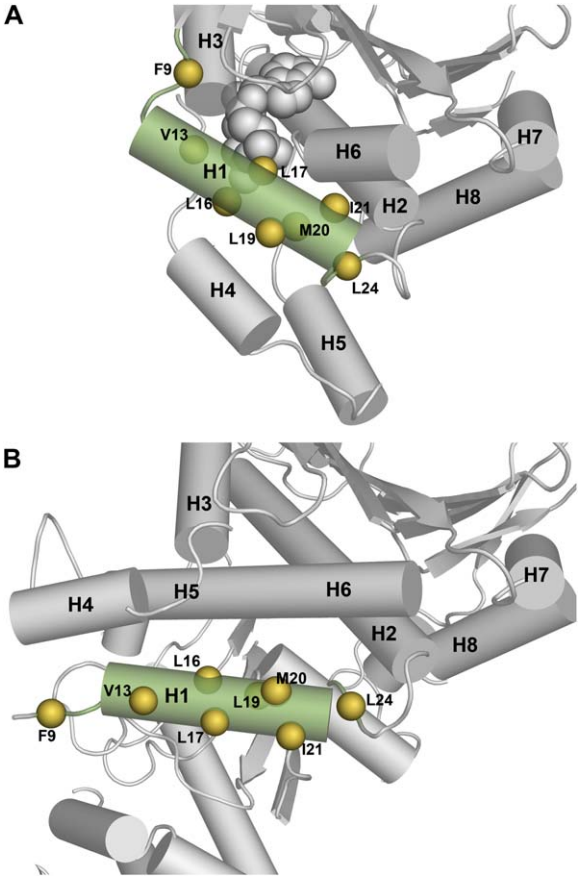

Figure 4. ADP Binding Alters the Exposure of NTD Hydrophobic Residues

(A) In the Mg^{2+}ADP bound isolated NTD (Figure 3B), nucleotide binding causes H1 to rotate by 180°, thereby burying most of the hydrophobic residues exposed in the apo structure against a hydrophobic face formed by the lid helices.

(B) In the apo full-length dimer, H1 (green) is oriented to expose a large patch of hydrophobic residues (F9, V13, L17, M20, L24—Cα positions marked by yellow spheres) into the binding cleft.

lid if the NTD/MD relationship remains constant (as in the HtpG NTD/MD fragment structure; Huai et al., 2005), or, alternatively, it can stabilize an ordered lid conformation that is incompatible with the NTD/MD relationship in the apo structure. In order to accommodate this, the NTD/MD configuration must rearrange. The nature of these changes is suggested by the effects of ADP binding on the full-length protein, which we will describe later.

Client Proteins Could Bind in the Large, Open Interdimer Cleft

In addition to their effects on nucleotide binding, the specific conformations of helix H1 and the lid in the full-length structure dramatically enhance the surface hydrophobicity of HtpG relative to the isolated domain. Largely due to the rotation of H1 and motions of H4 and H5, multiple large hydrophobic NTD residues (V13, L17, M20, I21) become solvent exposed in the full-length structure. These residues, along with F9 and L24, are clustered to form a hydrophobic stripe of approximately 6.5Å × 29Å on the surface of the NTD (Figure 4B). A crystal packing arrangement in which these residues are buried against the same hydrophobic residues from a symmetry-related molecule suggests that this NTD hydrophobic patch is capable of supporting protein/protein interactions and hence may have a role in client protein binding.

Along with the hydrophobic patch contributed by the NTD, exposed hydrophobic surfaces are also created by the MD src loop and the CTD helix H21 (Figure 2). As a consequence, each monomer of the open HtpG dimer presents three hydrophobic elements into the inner concave surface. Thus, the central cleft (~40–45 Å wide at the midpoint and ~30–35 Å deep) appears to be an ideal location for client protein binding (Figure 2). The H21s from the two CTDs lie at the base of this cleft spaced ~20 Å away from each other. The NTD lid region and the MD src loop from each protomer lie along one side of the cleft ~15–20 Å away from the H21 of the partner protomer. Although this configuration of hydrophobic elements does not resemble those presented by other chaperones, based on its size and surface character, we propose that it is this inside surface of the open apo state that preferentially engages client proteins.

ADP Induces Dramatic Conformational Rearrangements

To further elucidate the effects of ADP on the structure, HtpG bound to ADP was crystallized and the resulting structure determined to ~3.55 Å by molecular replacement using individual domain structures as search models (Experimental Procedures, Table S1). With the exception of local changes in the NTD active site lid and the MD src loop, the conformations of the individual domains do not change as a consequence of ADP binding. ADP is bound by the NTD in the full-length protein much as it is by the isolated domain, except that, because there is no Mg^{2+} ion in the full-length structure, the β phosphate adopts a distinct conformation.

In marked contrast to the subtle rearrangements observed in the published HtpG NTD/MD fragment structures (Huai et al., 2005), nucleotide binding to the intact protein dramatically alters both interdomain and intersubunit interactions. Each HtpG monomer bound to ADP adopts an extended, almost linear, conformation (hereafter referred to as the extended dimer; Figure 5A) in comparison to the curved, open apo conformation (Figure 2) or either of the compact conformations observed by EM (Figures 1B and1C). Based on superposition of the CTD, the MD in the presence of ADP is pivoted by 15° away from its position in the apo structure. More dramatically, the NTD is flipped up and away from the MD (~127° rotation), apparently exposing the nucleotide binding pocket (Figure S6E). In this extended structure, the NTD and MD are only associated via limited contacts between helices H2 and H3 from the NTD and one of the edges of the

first large α/β subdomain of the MD. These interactions bury a mere ~450 Å^2 of largely hydrophilic surface area as opposed to the ~1060 Å^2 buried in the apo structure. While the CTD dimerization interface is essentially unaffected by the presence of ADP, the motions within each monomer bring both the NTDs and MDs closer to each other. However, because the majority of the NTDs remain separated by ~30 Å in the dimer (Figure 5A), only the lid regions extend out from the domain to touch at their very tips (182 Å^2 over residues 106–112). Significant conformational changes in both the NTD lid and MD src loop are required to form even this glancing contact. The NTD lid adopts a conformation distinct from those observed in the isolated domain or full-length apo structures. In the ADP bound full-length structure, residues 99–108 and 112–116 form two nearly orthogonal helices that are oriented parallel to the plane of the NTD β sheet (Figure 3C). This structural transformation is linked to a set of previously unobserved intersubunit interactions.

Complementary Interactions between Hydrophobic Elements Stabilize a Crystallographic Dimer of Dimers

The crystallographic asymmetric unit is actually composed of two inverted and interlocking dimers (Figure 5B). This dimer of dimers is stabilized primarily by extensive interaction of the NTDs from one dimer with the MDs and CTDs of the other dimer. Specifically, each NTD is cradled against the first subdomain of an MD and lies on top of a CTD from the other protomer. The importance of this novel domain configuration is highlighted by both the size as well as the complementarity of the resulting interface (Figure 5C). All three domains bury an extraordinarily large amount of surface area (3736 Å^2/monomer total buried surface area), dwarfing the 1280 Å^2 buried by the protomers in the apo structure. Analysis of a large set of crystal structures shows that typical protein-protein interfaces are 1600 (±400) Å^2, whereas very large interfaces, such as this one, are between 2000–4660 Å^2 (Lo Conte et al., 1999).

The positioning and conformation of the NTD lids lie at the heart of this unprecedented domain rearrangement. Each of the NTD lids from one dimer is inserted into a channel bound by the MD src loops, the last domain of the MD (401–494) and the N-terminal end of the CTD helix H21s of the other dimer (Figure 5C). Remarkably, each NTD lid is within 5–10 Å of an MD src loop and a CTD H21. As a consequence, the key hydrophobic surfaces, which are completely exposed in the cleft of the nucleotide-free state, have coalesced to form a well-packed hydrophobic core for the dimer of dimers. This intimate interdigitation completely excludes these elements from solvent (Figure 5C). Although the modest resolution of the structure precludes precise analysis of sidechain interactions, no polar interactions are evident between the lids, src loops, and CTD helices. The limited sequence conservation within each of these three elements among hsp90s is perhaps a reflection of the specialized demands of different organisms for client-protein association. Nonetheless, the conserved hydrophobic character of these elements would likely support the same type of mutual packing and exclusion from solvent observed here.

DISCUSSION

We have determined the X-ray structures of full-length HtpG in two dramatically different conformations. Consistent with the EM data (Figure 1), in the absence of nucleotide, HtpG in the crystal adopts an open conformation in which each of the three domains of both monomers present a hydrophobic element into a large dimeric cleft (Figure 2). We believe this structure captures the enzyme poised to bind client proteins. In electron micrographs, ADP binding triggers dramatic conformational rearrangements that result in a highly compact state distinct from that induced by AMPPNP binding (Figure 1). While equally significant structural changes are evident in the ADP bound HtpG crystal structure, neither the observed extended dimer nor the dimer of dimers resembles the compact ADP state observed by electron microscopy. In addition, all available evidence suggests that only a dimer is required for proper hsp90 function. How do we resolve this apparent contradiction?

NTD Domain Swapping Could Lead to the Formation of a Compact, Nucleotide Bound Dimer

To resolve this problem, we propose a model for an isolated dimeric state that recapitulates all of the domain interactions observed in the crystal, and that is consistent with the EM observations of isolated dimers. Such a model can be constructed by a simple topological rearrangement of the domain connectivity in the crystallographic dimer of dimers. Close inspection of the structure (Figure S5) reveals that the C terminus of each NTD (residue 227) is roughly equidistant from the N terminus of its own MD (residue 233, 17 Å) and that of an MD in the partner dimer (23 Å). Given that the linker connecting the NTD and MD and the loop at the N terminus of the MD (residues 233–242) appear to be flexible, it seems that this region could readily accommodate either connection. This alternate linkage would allow the construction of a ''compact'' dimeric state (Figures 6A and 6B) that can be achieved by a ~60° rotation of the NTD from the apo state (Figure S6E; also see animation, Figure S7).

This modeled compact ADP conformation is entirely consistent with the size and shape of the ADP bound HtpG as seen in the electron micrographs and class averages (Figure 6C). Further, a recent crosslinking study of Grp94 uniquely supports this domain geometry with its highly complementary interleaving of hydrophobic elements (the NTD lid, the MD src loop, and the CTD H21). Specifically, interprotomer crosslinks were identified between lysine residues in the NTD and the MD as well as those between the MD and the CTD that are completely consistent with the domain positioning observed in the

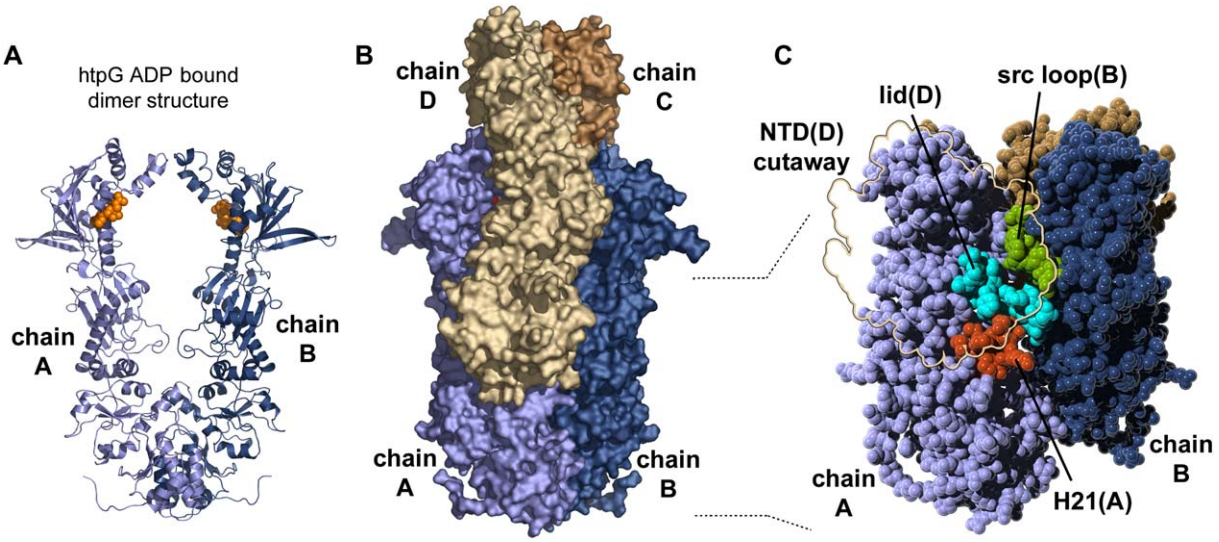

Figure 5. The ADP Bound Full-Length HtpG Forms a Dimer of Dimers Stabilized by an Intimate Hydrophobic Core

(A) The structure of ADP bound HtpG reveals an extended dimer showing minimal contact between NTDs, limited to the very tips of the lid regions. The bound ADPs (orange) are significantly exposed in the dimer. The necessary domain motions required to transition from the apo state to this state are shown in Figure S6E.

(B) The asymmetric unit of the crystal contains a tetramer composed of two interlocked, inverted dimers. The NTD lid regions of one dimer are inserted into a channel formed by the CTD helix (H21) and MD src loop of the alternate protomer.

(C) A cut-away view (NTD of the beige monomer removed as indicated by the beige outline) shows the intimate collapsed core of the compact dimer. The extent and complementarity of the very large interdomain interface (3736 $Å^2$/monomer) is shown. Hydrophobic elements from the NTD lid (blue), the MD "src loop" (green), and the CTD amphipathic H21 helices (orange) converge and become interdigitated within the core. These key hydrophobic elements are all exposed in the apo form (Figure 2).

dimer of dimers (Chu et al., 2006). The Cα-Cα distances for all of the equivalent residues in HtpG (Lys45-Thr343; Lys45-Arg346; Asp92-Arg346; Asp92-Arg349; Ala439-Ala555) are between 10.4 and 14.1 Å, well within reach of a lysine crosslink. Moreover, none of the NTD-MD residues are within crosslinking range in either the apo state, the extended ADP state, or the AMPPNP bound state of hsp82 (Ali et al., 2006).

The Active Site Lid Is a Nucleotide-Sensitive Conformational Switch

In non-hsp90 members of the GHKL family, the process of nucleotide hydrolysis requires that the NTD active site lid move from an inactive "lid-up" or disordered conformation to a "lid-down" conformation. As its name would suggest, the lid folds over the bound nucleotide during catalysis and functions much like the P loop motif of other ATPases (Ban and Yang, 1998; Corbett and Berger, 2005; Wigley et al., 1991). The N-terminal residues from the NTD of one protomer form a "strap" that lies across the outward face of the active-site lid of the other protomer, stabilizing the "lid-down" conformation. Hence, motions in the lid are coupled to the transient NTD-dimer interactions required for ATP hydrolysis in these proteins (Corbett and Berger, 2005; Wigley et al., 1991; Ban et al., 1999; Wegele et al., 2003).

Biochemical data and the structural homology between hsp90 and type II topoisomerases and MutL family members have suggested that ATP hydrolysis in hsp90 occurs by a similar mechanism. In particular, the lid-up conformation of all isolated hsp90-NTD structures (lid state 2; Figure 3B) and the lid-down conformation of the AMPPNP bound hsp82:p23 complex (lid state 3; Figure 3E) lend credence to this notion. The positioning of the lid and the NTD straps in the AMPPNP complex structure confirms that NTD dimerization is likely required for ATP hydrolysis as in other GHKL family members (Ali et al., 2006).

However, our structural data suggests that the role of the lid is far more complex, functioning as the central link between ATP binding/hydrolysis and client-protein binding/release. Beyond the lid-up and lid-down conformations, we observe two additional structural states of the lid. First, in our apo full-length HtpG structure, the lid adopts a position in which residues 121–124 sterically preclude nucleotide binding (lid state 1; Figure 3A). In this conformation, the lid (and the neighboring H1) exposes a hydrophobic face. Second, in our full-length ADP complex, the lid adopts a conformation in which it interacts extensively with the MD src loop and CTD H21, stabilizing a *trans*-protomer interaction (lid state 4; Figure 3C). Transitions between the four lid conformations not only involve positional motions but notable secondary structural alterations.

What is the purpose of these unique lid conformations? In type II topoisomerases and MutL, nucleotide binding is used to close the NTD dimer gate, which entraps one of

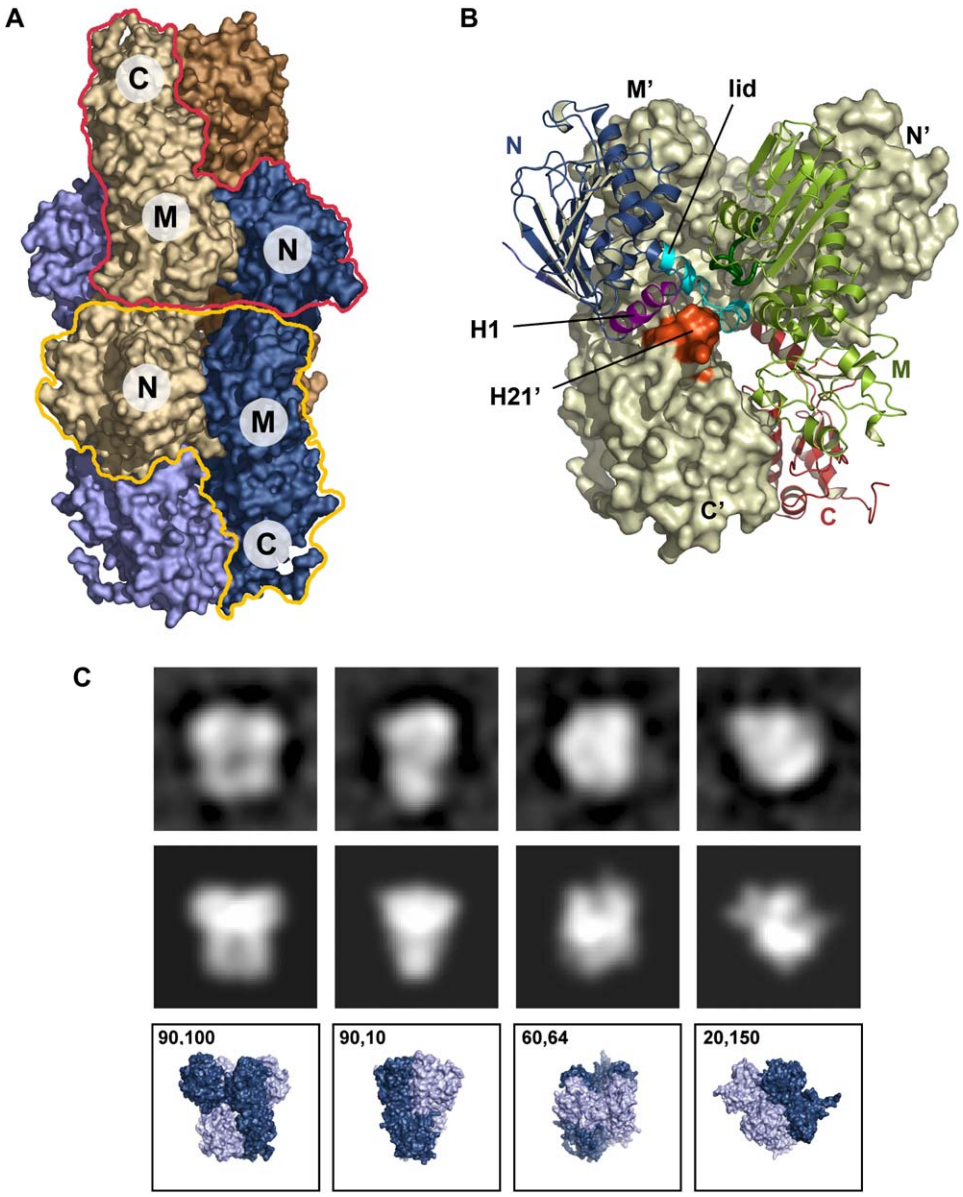

Figure 6. Model of the Compact Nucleotide Bound HtpG Dimer

(A) The outlines and domain labels delineate monomers of our proposed domain-swapped HtpG conformation in which the CTD and MD of one monomer are connected to the NTD from a monomer of the opposite inverted dimer, creating a compact dimer (see also Figure S6). A schematic diagram of the proposed topological change is shown in the inset (N = NTD, M = MD, and C = CTD).

(B) In this proposed compact dimer, the NTDs of each protomer are cradled on top of the MD and the CTD of the partner monomer. For the foreground protomer, the NTD is in blue, the MD in green and the CTD in red. The NTD lid (cyan) is inserted into a tunnel bound by H21 (red), the src loop (orange), and the third subdomain of the MD. In this configuration, H1 from the NTD lies on the face of the H21 of the partner protomer.

(C) The proposed compact dimer matches images obtained from EM (Figures 1 and S1) in both size and shape. As before, a set of 2D projections are calculated from the atomic model and matched to the reference-free EM class averages of htpG:ADP (top row, same as in Figure 1C). Matching views of the model (bottom row) and the 20 Å calculated projections from the model along with the orientation angles (middle row) are shown. The range of orientations indicate that the general shape agreement between the proposed compact model and the EM data is valid in three dimensions. The box width is 160 Å with 2.2 Å/pixel.

the target DNA strands. Gate closure is stabilized by interprotomer interactions between the NTD lids and straps. Hydrolysis is used as a timing mechanism and to ultimately reopen the gate (Ban et al., 1999; Corbett and Berger, 2005; Wegele et al., 2003; Wigley et al., 1991). In contrast, we propose that the fundamental role of the hsp90 active-site lid is to directly and indirectly couple ATP binding and hydrolysis to cyclical changes in domain

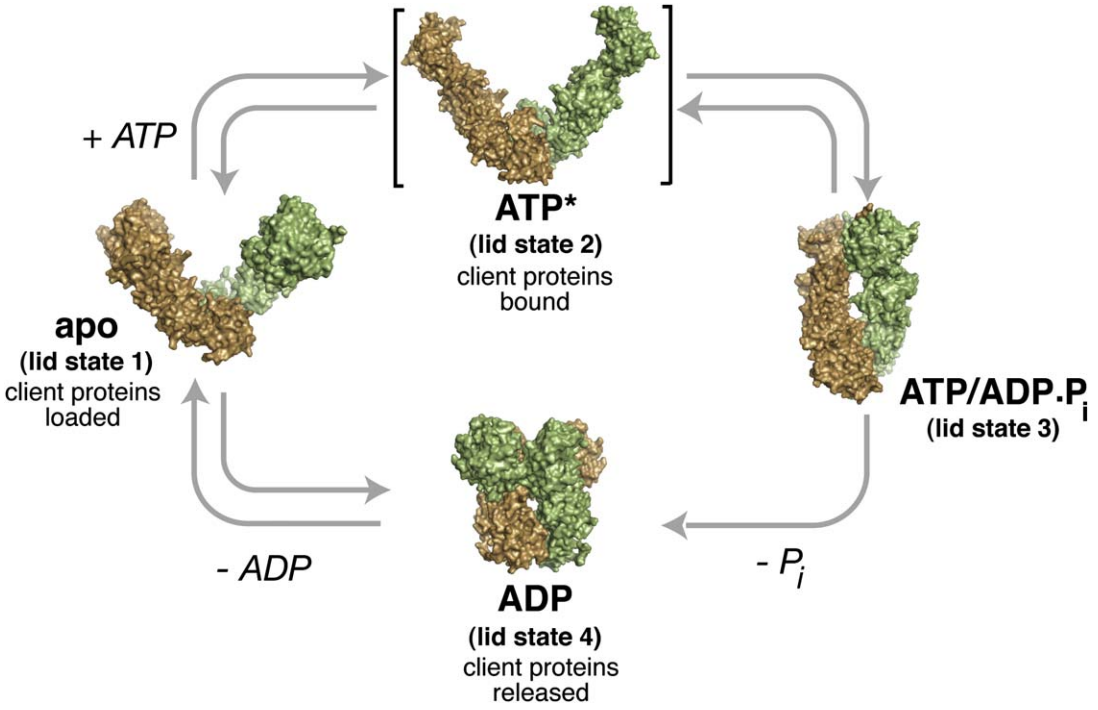

Figure 7. The hsp90 Chaperone Cycle

In the apo state, the NTD (blue), MD (green), and CTD (tan) each present hydrophobic surface area (orange) into the large interdomain cleft. This state is likely to be the most efficient at binding client proteins. Addition of ATP necessitates altering the relationship between the NTD and MD (Figures S4 and S6), resulting in a transient NTD/MD conformation (ATP*) perhaps like that observed in the extended ADP state (Figure 5B), yet having a lid organized more like in the isolated ADP NTD (state 2). Client proteins would remain bound due to the hydrophobic surfaces still present on the MD and CTD. This state then transitions to a more compact ATP state, as observed for HtpG by EM (Figure 1B) and the yeast AMPPNP structure (lid state 3) (Ali et al., 2006), which likely effects client-protein remodeling. Finally, nucleotide hydrolysis results in the very compact ADP state (lid state 4) that, because all the once-exposed hydrophobic elements are buried, would be expected to complete the release of client proteins and many cochaperones, thereby resetting the chaperone for another round.

organization and hydrophobic surface exposure and hence to client-protein binding and release.

A Model for the hsp90 Chaperone Cycle

The broad array of structural and functional data on hsp90s, including the work described here, can be rationalized in a chaperone cycle illustrated in Figure 7. Mammalian hsp90s have been demonstrated to bind and release their client proteins in a cyclic fashion. We suggest that the basic cycle is similar between the eukaryotic and bacterial hsp90s and consists of multiple states in equilibrium with directionality determined by ATP binding and hydrolysis. The cycle begins with the apo state, where the enzyme presents multiple hydrophobic elements into the central cleft, including the hydrophobic patch formed by one face of the active-site lid as well as helix H1 (Figures 2 and 4). The apo state, because it exposes the most hydrophobic surface area of all the states, is likely the most optimal for client-protein binding (especially in *E. coli,* which apparently lacks cochaperones). We surmise that the minimal MD/CTD interface is primarily responsible for the flexible positioning of these hydrophobic elements required to accommodate the diverse shapes and sizes of hsp90 client proteins (Figures 1 and S1).

In the apo state, the nucleotide binding cleft is occupied by the sidechain of Phe123 and the mainchain atoms of Gln122 and Phe 123, thereby hindering ATP access. We suggest that ATP binding would displace Phe123 and Gln122 and drive lid rearrangement to the more polar conformation observed in the isolated NTD structures. Because this lid conformation is incompatible with the NTD/MD relationship observed in the apo structure (Figure S4A), ATP binding would necessitate either the disordering of the lid (as observed in the NTD/MD fragment structure; Huai et al., 2005) or the reorientation of the NTD and MD. We postulate the existence of an ATP-containing intermediate state in which client proteins could be bound in a central cavity, however having an NTD/MD configuration that could resemble that observed in our extended dimer structure (Figures 5A and S6; ATP* in Figure 7). Alternatively, client-protein binding could disrupt the lid/src loop interactions observed in the apo state, which in turn would lead to an altered NTD/MD configuration (as in ATP*) that favors nucleotide binding. In either case, as a consequence of the lid rearrangement, the

overall surface hydrophobicity of the enzyme would decrease, but due to the continued exposure of the src loop and CTD helix H21, client proteins would still be expected to bind in this prehydrolysis intermediate.

Because ATP binding would disrupt or loosen the interaction between the NTD and MD, there would be an increased probability of sampling the conformation observed for the AMPPNP bound state of the yeast hsp90 (Figures 1B and S6D). In the AMPPNP bound yeast crystal structure (Ali et al., 2006), Arg380 (Arg336 in HtpG) from the MD hydrogen bonds with the γ-phosphate of the nucleotide. Hence, this residue clearly acts as an ATP sensor and may also have a role in hydrolysis. The lid adopts a conformation (state 3) distinct from that of either the apo full-length structure or the isolated NTD structure and covers the bound nucleotide (Figure 3). This once again exposes a hydrophobic face for the lid, which is now used to stabilize NTD dimerization via N-terminal residues (including residues from strand S1) from the partner protomer. Importantly, ATP-mediated closing of the interprotomer space could very well drive client-protein remodeling. As a consequence, affinity of hsp90 for client proteins would be reduced and presumably limited to interactions available on the sides of the molecule. However, in eukaryotes, the reduction in intrinsic affinity could be compensated by cochaperone/client-protein interactions (Kosano et al., 1998).

Once hydrolysis occurs, the interaction between Arg336 and the nucleotide would be broken and the protein would be able to sample the ADP bound compact, closed state. Here the lid assumes its fourth conformation, which has two functionally important consequences. First, it could act as a "gasket" to help seal the NTD against the MD, stabilizing the very compact configuration. Second, this lid conformation allows the interdigitation of the lid, the src loop, and the CTD H21, mutually masking their otherwise exposed hydrophobic surfaces in a newly formed, collapsed hydrophobic core (Figure 5C). This would assure complete release of client proteins from hsp90. Finally, nucleotide dissociation would be linked to opening the cleft and a subsequent round of client-protein binding. Thus, we propose that a distinct set of lid conformations is responsible for coupling nucleotide binding and hydrolysis to a cycle of domain rearrangements, which in turn regulate client-protein binding and release. Ultimately, using knowledge of the hsp90 chaperone cycle, it may be possible to identify small molecule compounds that selectively affect the different stages of the cycle, thereby affording more selective and potentially safer therapeutics.

Conclusion

Because the interrelationship between all three domains is both highly dynamic and central to function, it is perhaps not surprising that the complex domain interactions detailed here have not been revealed by either isolated domain or large fragment structures of hsp90s. Other chaperones such as GroEL and hsp70s amplify local changes induced by ATP binding and hydrolysis to large-scale domain rearrangements that reversibly mask client protein binding sites. The data we present here indicates that the hsp90 mechanism of action is also dictated by these same structural themes and involves at least three distinct conformational states.

EXPERIMENTAL PROCEDURES

Untagged, wild-type, mutant, and selenomethionine-labeled full-length *Escherichia coli* HtpG (residues 1–624), N-terminally 6XHis-tagged HtpG NTD (residues 1–215), and C-terminally 6XHis-tagged HtpG MD (residues 230–495) were expressed in *E. coli*, purified, and crystallized by hanging drop vapor diffusion as described in the Supplemental Experimental Procedures and Tables S1 and S2. X-ray diffraction data were collected at the ALS beamlines 8.2.1, 8.2.2, and 8.3.1, the CHESS beamline F1, and the SSRL beamline 1-5. The crystal structures of Mg^{2+}ADP NTD complex (R/R_{free} = 16.3%/19.8%) and the MD (R/R_{free} = 17.2%/22.5%) have been determined to 1.65 Å and 1.90 Å, respectively. The crystal structures of the apo full-length HtpG (R/R_{free} = 32.3%/37.0%) and the ADP/full-length HtpG complex (R/R_{free} = 32.0%/35.3%) have been determined to 3.50 Å and 3.55 Å, respectively.

For EM, HtpG was incubated, alone or with AMPPNP or ADP, placed on a carbon-coated grid and stained with uranyl formate, and imaged at 67,000× using an FEI Tecnai T20 EM. Image analysis was performed using EMAN (Ludtke et al., 1999). Full details are presented in the Supplemental Experiemental Procedures. Coordinates have been deposited for the isolated HtpG NTD (2IOR) and MD (2GQ0) as well as the full-length apo (2IOQ) and ADP (2IOP) structures.

Supplemental Data

Supplemental Data include six figures, one table, experimental procedures, references, and a movie and can be found with this article online at http://www.cell.com/cgi/content/full/127/2/329/DC1/.

ACKNOWLEDGMENTS

Funding for this project was provided by the Howard Hughes Medical Institute, NIH PO1 grant DK58390, and a UC Discovery Grant number bio03-10401. In the early stages of the project, A.K.S. was supported by a Howard Hughes Medical Institute Predoctoral Fellowship and a UCSF Chancellor's Fellowship. S.F.H. was supported by a Helen Hay Whitney Foundation Fellowship. We wish to thank H. Deacon, P. Foster, S. Hymowitz, P. Hwang, R. Keenan, R. Wagner, J. Ybe, and the staff at the Advanced Light Source (ALS) beamlines 8.2.1, 8.2.2, and 8.3.1, the Stanford Synchrotron Radiation Laboratory (SSRL) beamline 1-5 (particularly H. Bellamy), and the Cornell High Energy Synchrotron Source (CHESS) beamline F1 for support during data collection. We wish to especially thank C. Gross, A. Desai, L. Rice, C. Cunningham, and K. Krukenberg for many helpful discussions and comments on the manuscript. Finally, we would like to thank T. Mau for his unwavering support on multiple aspects of the project.

Received: March 11, 2006
Revised: August 13, 2006
Accepted: September 26, 2006
Published: October 19, 2006

REFERENCES

Ali, M.M., Roe, S.M., Vaughan, C.K., Meyer, P., Panaretou, B., Piper, P.W., Prodromou, C., and Pearl, L.H. (2006). Crystal structure of an Hsp90-nucleotide-p23/Sba1 closed chaperone complex. Nature *440*, 1013–1017.

Ban, C., and Yang, W. (1998). Crystal structure and ATPase activity of MutL: implications for DNA repair and mutagenesis. Cell *95*, 541–552.

Ban, C., Junop, M., and Yang, W. (1999). Transformation of MutL by ATP binding and hydrolysis: a switch in DNA mismatch repair. Cell *97*, 85–97.

Chiosis, G., Lucas, B., Huezo, H., Solit, D., Basso, A., and Rosen, N. (2003). Development of purine-scaffold small molecule inhibitors of Hsp90. Curr. Cancer Drug Targets *3*, 371–376.

Chu, F., Maynard, J.C., Chiosis, G., Nicchitta, C.V., and Burlingame, A.L. (2006). Identification of novel quaternary domain interactions in the Hsp90 chaperone, GRP94. Protein Sci. *15*, 1260–1269.

Corbett, K.D., and Berger, J.M. (2005). Structural dissection of ATP turnover in the prototypical GHL ATPase TopoVI. Structure *13*, 873–882.

Dutta, R., and Inouye, M. (2000). GHKL, an emergent ATPase/kinase superfamily. Trends Biochem. Sci. *25*, 24–28.

Dymock, B.W., Barril, X., Brough, P.A., Cansfield, J.E., Massey, A., McDonald, E., Hubbard, R.E., Surgenor, A., Roughley, S.D., Webb, P., et al. (2005). Novel, potent small-molecule inhibitors of the molecular chaperone Hsp90 discovered through structure-based design. J. Med. Chem. *48*, 4212–4215.

Feltham, J.L., and Gierasch, L.M. (2000). GroEL-substrate interactions: molding the fold, or folding the mold? Cell *100*, 193–196.

Freeman, B.C., and Yamamoto, K.R. (2002). Disassembly of transcriptional regulatory complexes by molecular chaperones. Science *296*, 2232–2235.

Grantcharova, V., Alm, E.J., Baker, D., and Horwich, A.L. (2001). Mechanisms of protein folding. Curr. Opin. Struct. Biol. *11*, 70–82.

Harris, S.F., Shiau, A.K., and Agard, D.A. (2004). The crystal structure of the carboxy-terminal dimerization domain of htpG, the Escherichia coli Hsp90, reveals a potential substrate binding site. Structure (Camb) *12*, 1087–1097.

Horst, R., Bertelsen, E.B., Fiaux, J., Wider, G., Horwich, A.L., and Wuthrich, K. (2005). Direct NMR observation of a substrate protein bound to the chaperonin GroEL. Proc. Natl. Acad. Sci. USA *102*, 12748–12753.

Huai, Q., Wang, H., Liu, Y., Kim, H.Y., Toft, D., and Ke, H. (2005). Structures of the N-terminal and middle domains of E. coli Hsp90 and conformation changes upon ADP binding. Structure *13*, 579–590.

Jez, J.M., Chen, J.C., Rastelli, G., Stroud, R.M., and Santi, D.V. (2003). Crystal structure and molecular modeling of 17-DMAG in complex with human Hsp90. Chem. Biol. *10*, 361–368.

Kosano, H., Stensgard, B., Charlesworth, M.C., McMahon, N., and Toft, D. (1998). The assembly of progesterone receptor-hsp90 complexes using purified proteins. J. Biol. Chem. *273*, 32973–32979.

Lo Conte, L., Chothia, C., and Janin, J. (1999). The atomic structure of protein-protein recognition sites. J. Mol. Biol. *285*, 2177–2198.

Ludtke, S.J., Baldwin, P.R., and Chiu, W. (1999). EMAN: semiautomated software for high-resolution single-particle reconstructions. J. Struct. Biol. *128*, 82–97.

Maruya, M., Sameshima, M., Nemoto, T., and Yahara, I. (1999). Monomer arrangement in HSP90 dimer as determined by decoration with N and C-terminal region specific antibodies. J. Mol. Biol. *285*, 903–907.

Mayer, M.P., and Bukau, B. (2005). Hsp70 chaperones: cellular functions and molecular mechanism. Cell. Mol. Life Sci. *62*, 670–684.

Meyer, P., Prodromou, C., Hu, B., Vaughan, C., Roe, S.M., Panaretou, B., Piper, P.W., and Pearl, L.H. (2003). Structural and functional analysis of the middle segment of hsp90: implications for ATP hydrolysis and client protein and cochaperone interactions. Mol. Cell *11*, 647–658.

Neckers, L., and Ivy, S.P. (2003). Heat shock protein 90. Curr. Opin. Oncol. *15*, 419–424.

Picard, D. (2002). Heat-shock protein *90*, a chaperone for folding and regulation. Cell. Mol. Life Sci. *59*, 1640–1648.

Pratt, W.B., and Toft, D.O. (2003). Regulation of signaling protein function and trafficking by the hsp90/hsp70-based chaperone machinery. Exp. Biol. Med. (Maywood) *228*, 111–133.

Prodromou, C., Roe, S.M., O'Brien, R., Ladbury, J.E., Piper, P.W., and Pearl, L.H. (1997). Identification and structural characterization of the ATP/ADP-binding site in the Hsp90 molecular chaperone. Cell *90*, 65–75.

Richter, K., and Buchner, J. (2001). Hsp90: chaperoning signal transduction. J. Cell. Physiol. *188*, 281–290.

Richter, K., Moser, S., Hagn, F., Friedrich, R., Hainzl, O., Heller, M., Schlee, S., Kessler, H., Reinstein, J., and Buchner, J. (2006). Intrinsic inhibition of the Hsp90 ATPase activity. J. Biol. Chem. *281*, 11301–11311.

Roe, S.M., Prodromou, C., O'Brien, R., Ladbury, J.E., Piper, P.W., and Pearl, L.H. (1999). Structural basis for inhibition of the Hsp90 molecular chaperone by the antitumor antibiotics radicicol and geldanamycin. J. Med. Chem. *42*, 260–266.

Stebbins, C.E., Russo, A.A., Schneider, C., Rosen, N., Hartl, F.U., and Pavletich, N.P. (1997). Crystal structure of an Hsp90-geldanamycin complex: targeting of a protein chaperone by an antitumor agent. Cell *89*, 239–250.

Wegele, H., Muschler, P., Bunck, M., Reinstein, J., and Buchner, J. (2003). Dissection of the contribution of individual domains to the ATPase mechanism of Hsp90. J. Biol. Chem. *278*, 39303–39310.

Whitesell, L., and Lindquist, S.L. (2005). HSP90 and the chaperoning of cancer. Nat. Rev. Cancer *5*, 761–772.

Wigley, D.B., Davies, G.J., Dodson, E.J., Maxwell, A., and Dodson, G. (1991). Crystal structure of an N-terminal fragment of the DNA gyrase B protein. Nature *351*, 624–629.

Workman, P. (2004). Altered states: selectively drugging the Hsp90 cancer chaperone. Trends Mol. Med. *10*, 47–51.

Young, J.C., Agashe, V.R., Siegers, K., and Hartl, F.U. (2004). Pathways of chaperone-mediated protein folding in the cytosol. Nat. Rev. Mol. Cell Biol. *5*, 781–791.

Young, J.C., Moarefi, I., and Hartl, F.U. (2001). Hsp90: a specialized but essential protein-folding tool. J. Cell Biol. *154*, 267–273.

Zhao, R., Davey, M., Hsu, Y.C., Kaplanek, P., Tong, A., Parsons, A.B., Krogan, N., Cagney, G., Mai, D., Greenblatt, J., et al. (2005). Navigating the chaperone network: an integrative map of physical and genetic interactions mediated by the hsp90 chaperone. Cell *120*, 715–727.

Zhu, X., Zhao, X., Burkholder, W.F., Gragerov, A., Ogata, C.M., Gottesman, M.E., and Hendrickson, W.A. (1996). Structural analysis of substrate binding by the molecular chaperone DnaK. Science *272*, 1606–1614.